JOURNAL OF MATERIALS SCIENCE 31 (1996) 6469–6476

Effect of boron-doping on structure and some properties of carbon–carbon composite

T. SOGABE*, K. NAKAJIMA, M. INAGAKI
*Faculty of Engineering, Hokkaido University, Kita-ku, Sapporo 060, Japan, and *also *Ohnohara Technical Development Centre, Toyo Tanso Co., Ltd. Ohnohara-cho Mitoyo-gun, Kagawa-ken 769-16, Japan*

Boron-doped carbon–carbon composites with boron concentration around 11–15 mass % were prepared from a carbon fibre felt with dispersed boron carbide powder by infiltration of pyrolytic carbon. The composite was heat treated at several different temperatures from 2000–2800 °C. The highest bending strength was obtained for the composite at a heat-treatment temperature (HTT) of 2200 °C. Carbon fibre began to be destroyed after heat treatment at 2400 °C and the structure of the composite was drastically changed above 2600 °C where the anisotropy of the composite originally existing in the thermal expansion coefficient and the thermal conductivity has been faded away. X-ray diffraction measurement indicated that graphitization of the composite was enhanced by boron doping. At HTTs above 2400 °C, the composite became graphitic, the crystallite sizes of which were more than 100 nm in L_c (0 0 4) and L_a (1 1 0). It was shown that boron was uniformly distributed in the composite at an HTT of 2400 °C and also that heat treatment at higher temperatures, such as 2600 °C, incurred condensation of boron. Air-oxidation loss at 800 °C appeared to be the lowest for the composite with an HTT of 2400 °C and the rate of oxidation loss was 22 times lower than that of the non-boron-doped composite.

1. Introduction

Quite a few fundamental studies of boron-doping into carbon materials have been conducted [1–8] and report that boron-doping enhances graphitization and reduces the gasification rate of carbon in air at high temperatures. Consequently, the application of a carbon–boron system for anti-oxidation refractory materials has been expected. Boron-doping into carbon materials has also been investigated to obtain neutron-absorbing materials for gas-cooled reactors [9–11]. Recently, studies of boron-doping into carbon materials have been actively carried out for the first wall or plasma-facing material of nuclear fusion devices [12–17]. For these engineering applications, some kinds of boron-doped engineering materials, composed of boron carbide and graphite, have been developed [18–20]. Even advanced materials have been demanded in recent technology, so that fabrication of a boron-doped material with a carbon fibre-reinforced carbon composite (C–C composite) that is commonly recognized to have high thermomechanical properties, has been considered. Although a few approaches to the fabrication of boron-doped C–C composites have recently been tried [21, 22], much more investigation will be necessary to meet engineering requirements. In this regard, we have tried to prepare a boron-doped C–C composite using a carbon-fibre felt and boron carbide powder as starting materials and by densification with pyrolytic carbon.

In the present work, the effect of boron-doping on the structure and some properties of the composites heat treated at high temperatures, was investigated.

2. Experimental procedure

2.1. Preparation of boron-doped C–C composite

For fabrication of a boron-doped felt carbon fibre-reinforced carbon composite (boron-doped C–C composite), boron carbide powder with the average grain size of 3 μm diameter, and a mesophase pitch-based carbon fibre felt, were used as starting materials. The size of the carbon felt sheet used for this fabrication was about $150 \times 60\ mm^2$ with a thickness of about 5 mm. A slurry of boron carbide powder with methyl alcohol was permeated into a carbon felt sheet, and the alcohol was evaporated at 120 °C over several hours. The preform was prepared by stacking 12 carbon felt sheets with boron carbide in order to produce some thickness in the composite for actual use. The amount of boron carbide in the slurry was determined to have a boron concentration around 15 mass % in the material after densification. The preform was densified with pyrolytic carbon by chemical vapour

*Author to whom all correspondence should be addressed.

0022–2461

infiltration up to its density around 1.7 g cm^{-3} and then heat treated at 2000, 2200, 2400, 2600 and 2800 °C using an Acheson-type furnace in an inert atmosphere, and the temperature was measured using a pyrometer. For comparison, a non-boron-doped C–C composite, having the same carbon-fibre felt and pyrolytic carbon matrix, was also prepared with a final heat-treatment temperature of 2800 °C.

The boron concentration of the boron-doped C–C composites was determined by chemical analysis. On the composites thus prepared, the directions are defined as the felt stacking direction, Z, the other two directions being X and Y. The length of 150 mm in the perform corresponds to the Y-direction.

2.2. Characterization of structure and texture

The microtexture of the composites and their boron distribution were studied using an electron probe microanalyser (EPMA, Jeol Model JXA-8900M). Each sample was mounted in a resin block and the surface of the sample was polished to have sufficient flatness for the observation. Pore distribution of the composites was measured using a mercury porosimeter (Carlo Erba Instrument Inc. Model 2000).

X-ray powder diffractometry was conducted for structural characterization of the materials using CuK_α radiation (Rigaku, Model CN2013). Lattice constants, c_0 and a_0, and apparent crystallite sizes, L_c, L_a and $L_{1\,1\,2}$, of the composites were determined from 0 0 4, 1 1 0 and 1 1 2 diffraction peaks, followed by a standard in Japan, the *Gakushin* method [23]. 0 0 8 diffraction peaks of the materials were also measured.

2.3. Measurement of physical properties and oxidation loss

Bending strength was measured by a three-point bending method with a span of 40 mm using a rectangular specimen with a size $6 \times 6 \times 60$ mm^3. In the measurement, the Y-direction corresponds to the length of 60 mm of the specimen and the load was applied parallel to the Z-direction. The thermal expansion coefficient in three directions was determined in the temperature range 25–1000 °C using a quartz bar as a reference. Thermal conductivity was also measured at room temperature by the laser flush method using a ruby laser.

For measurement of oxidation loss, a rectangular test specimen with a size of $32 \times 20 \times 12.5$ mm^3 was prepared and set in a resistance furnace [20]. After reaching the temperature to be tested, dry air was introduced at a flow rate of 2 l min^{-1}. The temperature was controlled within 5 °C of the setting point. After completing the oxidation, nitrogen gas was introduced into the furnace instead of air, for cooling down to near room temperature to allow measurement of the weight of the specimen. Oxidation loss (mass %) by air was calculated from the weight of the specimen before and after oxidation.

3. Results and discussion

3.1. Microtexture

The prepared samples, with their boron concentrations and bulk densities, are tabulated in Table I. We have tried to dope at least 10 mass % boron into each final composite, because it has been reported [19, 20] that around 10–15 mass % boron is necessary to produce an appreciable resistance to air-oxidation. About 11 mass % boron remained in the composite after heat treatment at 2800 °C, even though the boron concentration decreases with increasing heat-treatment temperature (HTT). X-ray diffraction profiles of the composites also suggest the presence of B_4C. Bulk density became a little lower after heat treatment at 2800 °C.

Scanning electron micrographs and boron-mapping pictures of the same view of the X–Y plane of boron-doped C–C composites are shown in Fig. 1. Fibres appear to be preferentially oriented parallel to the X–Y plane. Some SEM observations on the the X–Y plane of the composites supported this orientation of carbon fibres. For the composites heat treated at 2000 and 2200 °C in Fig. 1a and c, carbon fibres with a diameter of about 7 μm are seen, and pyrolytic carbon is deposited on carbon fibres with a thickness of nearly 15 μm. Localized large boron-rich areas, indicative of the mass of boron carbide, are seen in these composites (Fig. 1b and d). Boron is also seen in the carbon part in these composites, suggesting the diffusion of boron into the carbon or solid solution phase. By comparison of Fig. 1b and d, it is noted that boron diffusion is apparently promoted at an HTT of 2200 °C. These observations are consistent with the results reported by Lowell [2] that the solubility limit of boron into carbon is 1.50 and 2.05 at % at 2000 and 2200 °C, respectively.

For the boron-doped C–C composite at an HTT of 2400 °C, it is observed from Fig. 1e and f that some fibres are destroyed and the surrounding matrices begin to combine with each other, and that the masses of boron carbide are spread over the material, boron distribution becoming quite uniform. Such a uniform distribution of boron is considered to be attained by the active transportation of boron, caused by melting and vaporization of boron carbide, because there is a liquid phase at 2350 °C in the carbon–boron system [2] and it is considered that boron vaporizes rather easily at such a high temperature [17]. Some

TABLE I Carbon fibre felt-carbon composites prepared

Sample code	Heat-treatment temperature (HTT) (°C)	Bulk density (g cm^{-3})	Boron concentration mass %
Boron-doped			
a	2000	1.75	14.5
b	2200	1.70	13.5
c	2400	1.70	12.3
d	2600	1.68	11.7
e	2800	1.57	11.2
Non-boron-doped			
f	2800	1.70	0.0

rearrangement, followed by combining with the matrix, may assist the uniform distribution of boron.

At HTTs of 2600 and 2800 °C, in Fig. 1g and i, large crystalline grains are observed as a consequence of combining fibre and matrix, following the disappearance of fibres. In Fig. 1h and j, a localized high concentration of boron is also seen, indicating that boron, once spread, has condensed again at these high HTTs.

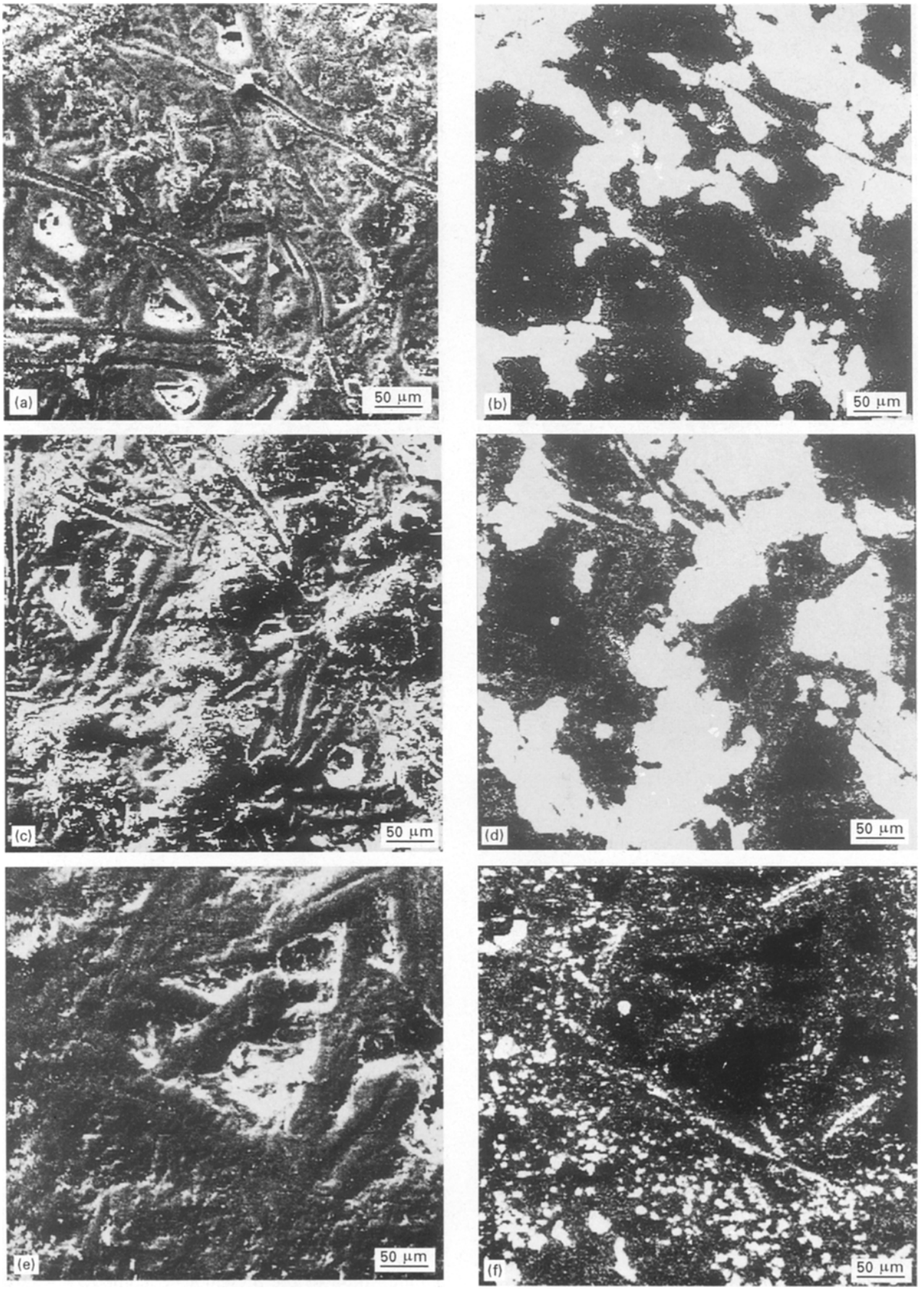

Figure 1 (a, c, e, g, i) Scanning electron micrographs and (b, d, f, h, j) boron-mappings of the polished surfaces of boron-doped C–C composites with various HTTs: sample a, at 2000 °C; sample b, at 2200 °C; sample c, at 2400 °C; sample d, at 2600 °C; sample e, at 2800 °C.

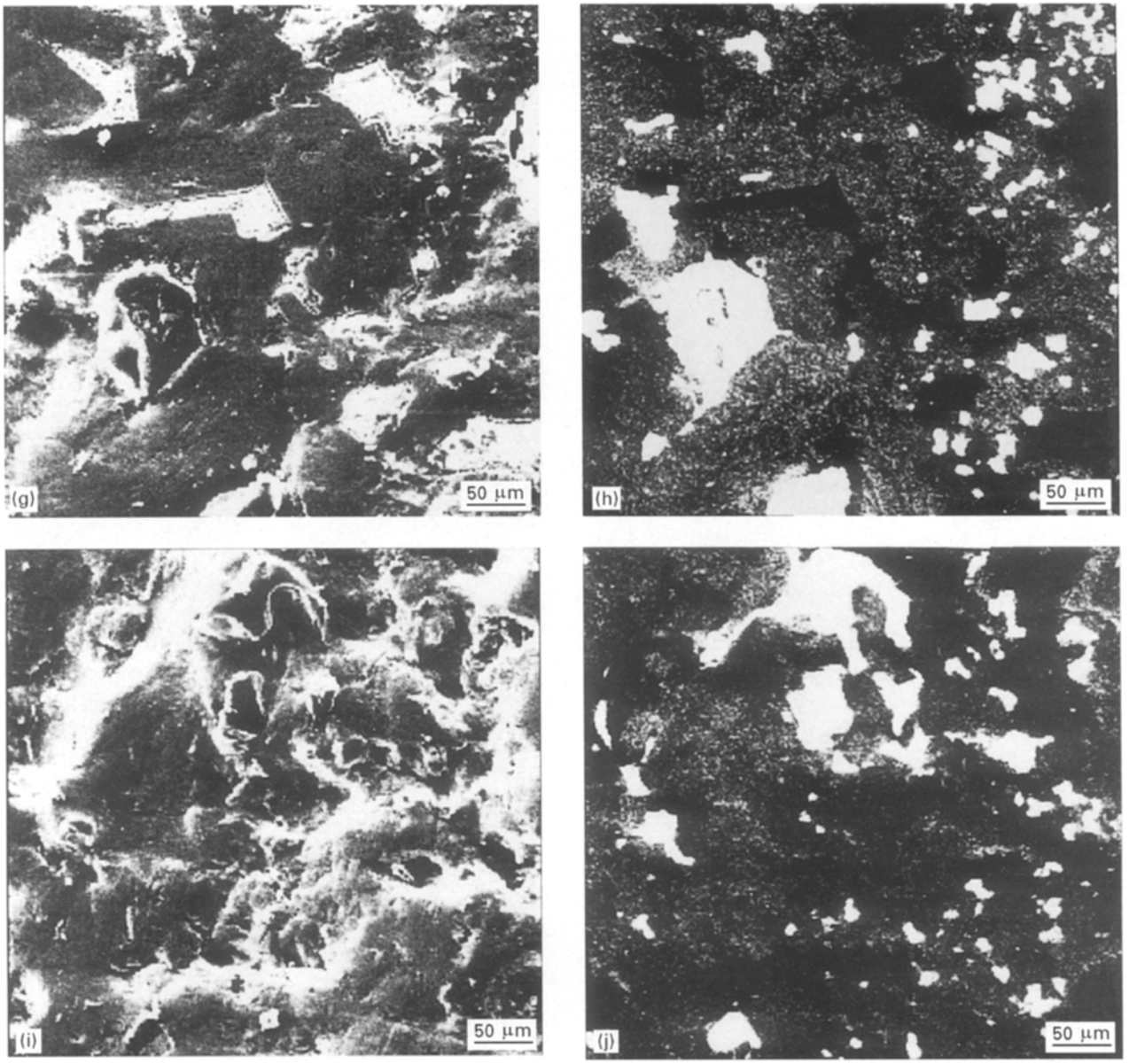

Figure 1 continued.

The mechanism of such a redistribution of boron is not known yet, but it should be noticed that the viscosity of molten boron carbide became low enough to flow so smoothly that boron could accumulate again. In a non-boron-doped composite heat treated 2800 °C, fibres and the surrounding matrix are clearly observed.

Pore-distribution curves for boron-doped C–C composites are shown in Fig 2. The changes in structure and boron distribution of the composites described above are well reflected in pore distributions of the composites. Pores are mostly in the range 5–20 μm for the composite at an HTT of 2000 °C, and there is no significant change in pore distribution or pore volume for the composite at an HTT of 2200 °C, as no significant difference was observed in the optical micrograph. At an HTT of 2400 °C, the pores with radius in the range 5–20 μm increase and pores with radius less than 0.2 μm are formed. On further heat treatment or at 2600 and 2800 °C, the large pores with radius of about 5–20 μm are much reduced to even less than that of an HTT of 2000 and 2200 °C, and small pores with radius less than 0.3 μm greatly increase. The transportation of boron carbide may greatly reflect these changes of pore distribution. At a temperature of 2400 °C, it is speculated that the segregation of the boron carbide creates the large pores and the vaporized boron carbide remains in small pores. At high temperatures, 2600 and 2800 °C, it is considered that the condensation of boron carbide and the rearrangement of the crystal domains reduce the volume of large pores, and further vaporization of boron increases the number of small pores.

3.2. Structure

The lattice constants and crystallite sizes of the composites are tabulated in Table II. X-ray diffraction profiles in the 2θ ranges of 81°–86° and 131°–135°, including 1 1 2, 1 0 5 and 0 0 8 lines, are shown in Fig. 3. These X-ray diffraction data show clearly that graphitization of the present C–C composite is enhanced by the catalytic action of boron, as reported by other authors [6, 7]. Clear, sharp peaks of 1 1 2 and

0 0 8 diffraction appear at HTTs above 2400 °C although only broad peaks are obtained for the non-boron-doped composite which has been heat treated at 2800 °C. Also, the 1 0 5 diffraction peak can be seen in the vicinity of the 1 1 2 peak only for the boron-doped C–C composites at HTTs above 2400 °C. Colour change observed by the eye on the boron-doped C–C composites, supported the X-ray diffraction analysis; while materials heat treated at 2000 and 2200 °C appeared black, those heat treated above 2400 °C exhibited a metallic lustre and even more lustring than the non-boron-doped composite heat treated at 2800 °C. The apparent crystallite sizes, L_a(1 1 0) and L_c(0 0 4) for the boron-doped C–C composites heat treated above 2400 °C, are more than 100 nm. The crystallite size, $L_{1\,1\,2}$, calculated from the half-width of 1 1 2 diffraction peak, is a measure of the thickness of three-dimensional graphitic stacking. The $L_{1\,1\,2}$ value of the boron-doped C–C composite at an HTT of 2400 °C is 20 nm, being one order larger than that at 2200 °C and also much larger than 6 nm for the non-boron-doped at HTT of 2800 °C. Such a high degree of graphitic stacking obtained for these composites may be responsible for the formation of large crystal grains as the result of combining and recrystallization of the fibre and matrix brought by catalytic action of boron, as seen in Figs. 1e, g and i. The lattice constants obtained for the present composites, c_0 (0 0 4), decrease with increasing of HTT up to 2400 °C, and level off on further heat treatment, and a_0 increases slightly at HTTs of 2600 and 2800 °C. Boron-doping at high HTTs also causes, in the present study, smaller c_0 and larger a_0 values than those of ideal graphite crystal, as

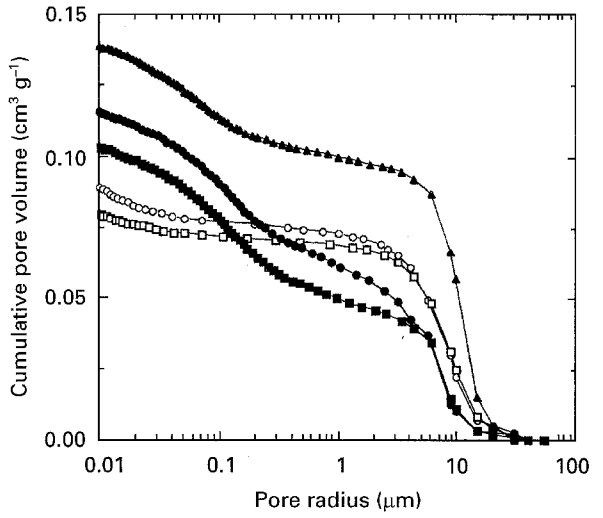

Figure 2 Pore-distribution curves of boron-doped C–C composites with various HTTs. (○) 2000 °C, (□) 2200 °C, (▲) 2400 °C, (■) 2600 °C, (●) 2800 °C.

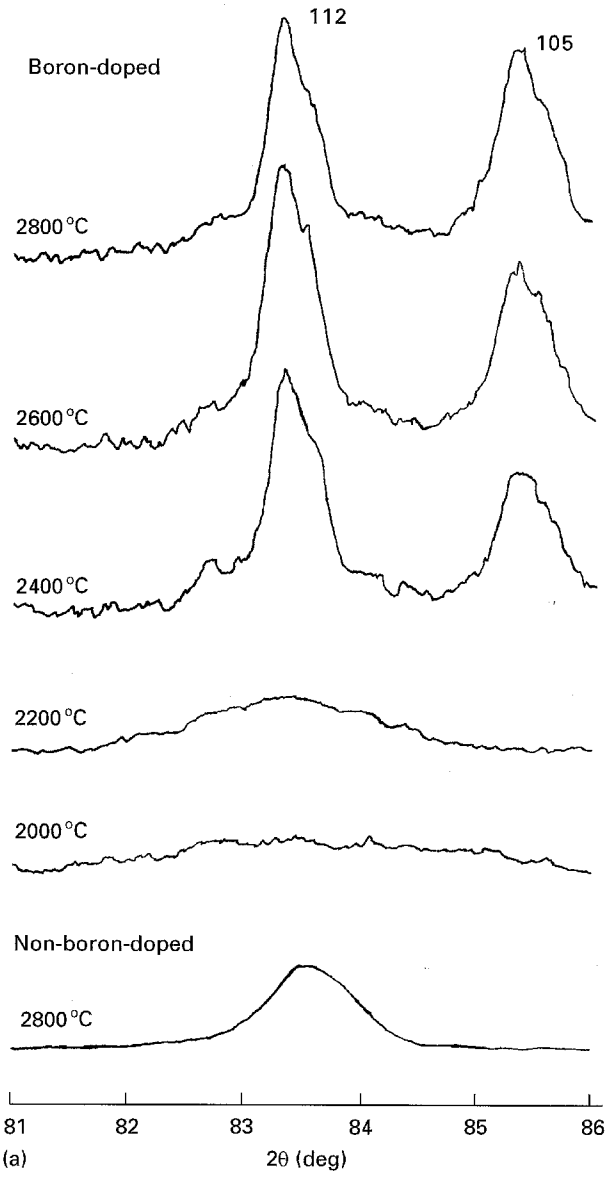

Figure 3 X-ray diffraction profiles of (a) 1 1 2 and 1 0 5 lines, and (b) 0 0 8 lines of boron-doped C–C composites with various HTTs.

TABLE II Lattice constants and crystallite sizes of C–C composites with various heat-treatment temperatures (HTT)

Sample code	HTT (°C)	Lattice constants		Crystallite sizes		
		c_0(0 0 4) (nm)	a_0(1 1 0) (nm)	L_c(0 0 4) (nm)	L_a(1 1 0) (nm)	$L_{(1\,1\,2)}$ (nm)
Boron-doped						
a	2000	0.6807	0.2461	9	25	0
b	2200	0.6759	0.2463	12	44	2
c	2400	0.6701	0.2462	> 100	> 100	20
d	2600	0.6701	0.2468	> 100	> 100	19
e	2800	0.6696	0.2468	> 100	> 100	28
Non-boron-doped						
f	2800	0.6724	0.2460	64	> 100	6

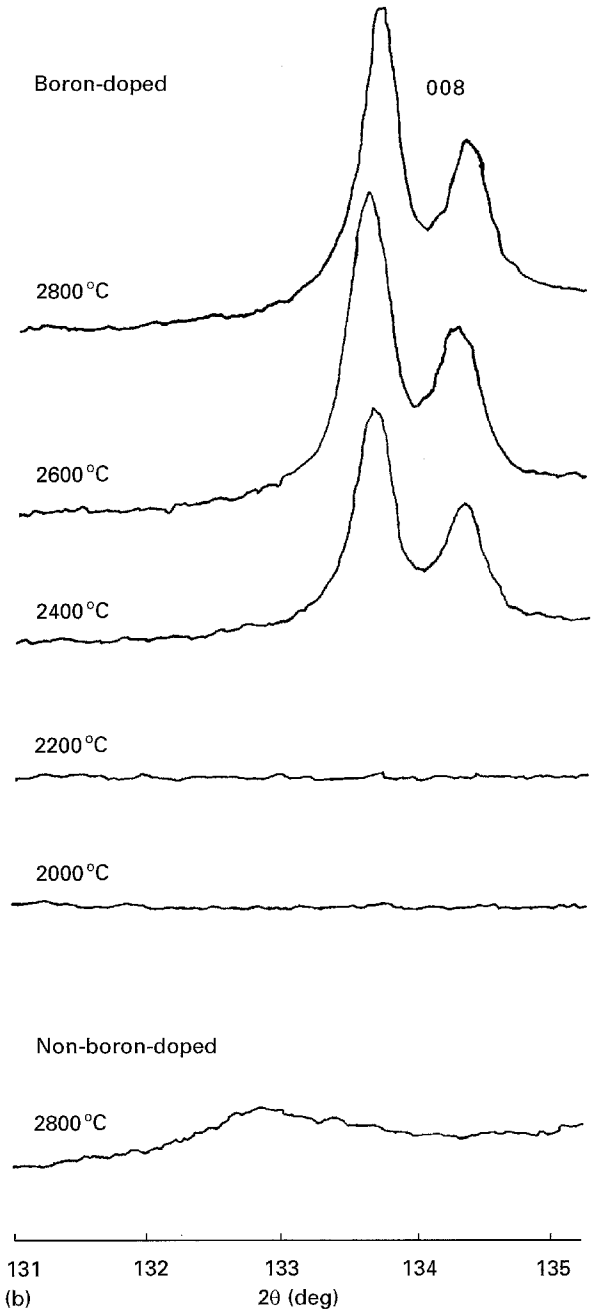

Figure 3 continued.

was reported [24] for the 0.6 mass % boron doping into natural graphite.

3.3. Physical properties and air-oxidation loss

Change in bending strength of boron-doped C–C composite with HTT is shown in Fig. 4. Bending strength slightly increases with increasing HTT from 2000–2200 °C. This finding can probably be attributed to the increased diffusion of boron into carbon at 2200 °C, as shown in Fig. 1b and d, which resulted in increased binding among matrices and between matrix and fibres. The bending strength of boron-doped composite at an HTT of 2200 °C is about 1.5 times higher than that of the non-boron-doped at HTT of 2800 °C, as shown in Fig. 4. Low bending strength of the composites heat treated above 2400 °C may be due to the formation of large crystalline grains and destruction of fibres in the materials, which allows easy shear crack propagation.

Change in the thermal expansion coefficient of boron-doped C–C composite for three directions with HTT is shown in Fig. 5. The coefficient along the Z-direction, the stacking direction of the felt sheets, has a larger value than those of the X- and Y-directions because of preferential orientation of carbon fibres, as shown in Fig. 1. The thermal expansion coefficients of the X- and Y-directions decrease slightly with increasing HTT from 2000–2400 °C, but that of the Z-direction increases from 2000–2200 °C and then begins to decrease. These changes are mainly attributed to the promoted graphitization around 2000–2400 °C, as shown in Table II and Fig. 3, which normally leads to decrease of the thermal expansion coefficient in the direction of parallel to the basal plane, and increase in the direction perpendicular to the basal plane [25]. The reduction of the thermal

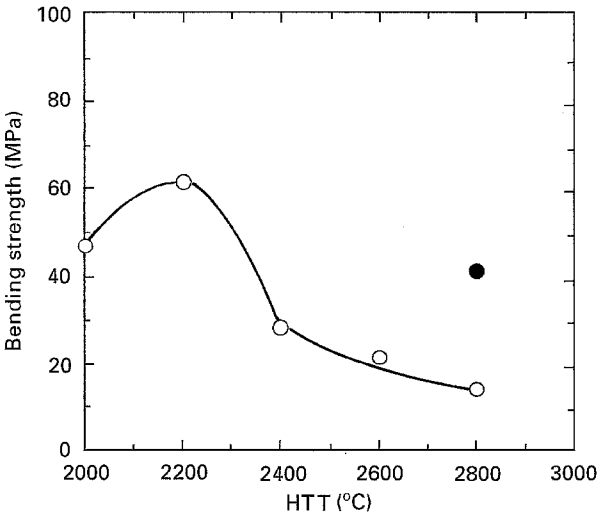

Figure 4 Effect of HTT on bending strength of C–C composite: (○) boron-doped, (●) non-boron-doped.

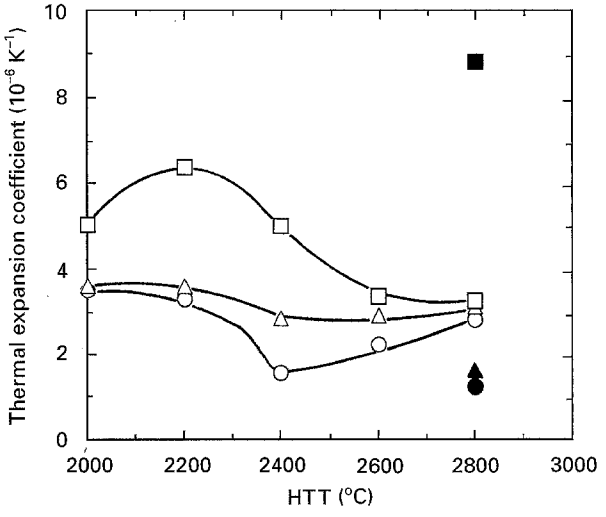

Figure 5 Effect of HTT on thermal expansion coefficient of the (○, ●) X-, (△, ▲) Y- and (□, ■) Z-directions of the C–C composite: (○, △, □) boron-doped, (●, ▲, ■) non-boron-doped. (Measured temperature range 25–1000 °C).

expansion of the composite for the Z-direction at HTT from 2200–2400 °C in spite of high degree of graphitization, is considered to be the effect of the structural change; damage of the fibre and the rearranged matrix lessens the orientation of the crystal. Anisotropy of the composite becomes smaller as the HTT increases from 2400–2800 °C, almost complete isotropy being obtained at 2800 °C, which indicates that the crystals are oriented in a random fashion as a consequence of the recrystallization of the fibre and matrix. Fairly large anisotropy is observed for the thermal expansion coefficient of non-boron-doped composite at an HTT of 2800 °C, as shown in Fig. 5. However, the average value of the three directions between boron-doped and non-boron-doped are nearly the same.

Change in thermal conductivity of boron-doped C–C composite for three directions with HTT is shown in Fig. 6. The highest thermal conductivity is observed at an HTT of 2200 °C for the X- and Y-directions, and it increases up to an HTT of 2400 °C for the Z-direction. Thermal conductivity in boron-doped composites is considered to be dominantly determined from the degree of graphitization and formation of carbon–boron solid solution; the former may promote a high thermal conductivity and the latter may decrease it due to the increased scattering of phonons [26]. Therefore, one may postulate that the peaks of thermal conductivity observed for the X- and Y-directions and the increase for the Z-direction, are a result of the competition between acceleration of graphitization and increase in phonon scattering brought about by the incorporation of boron into hexagonal planes. A slight increase in thermal conductivity seen in the Z-direction, unlike the other two directions, from an HTT of 2200–2400 °C may be the effect of the lessened crystal orientation as already stated. Because the formation of a solid solution has a large reducing effect, thermal conductivity of the composite apparently reduces in total, although the graphitization still proceeds between 2200 and 2400 °C. The fact that the anisotropy of thermal conductivity faded away on heat treatment above 2400 °C, also supports the view that the crystals are oriented randomly in the composite.

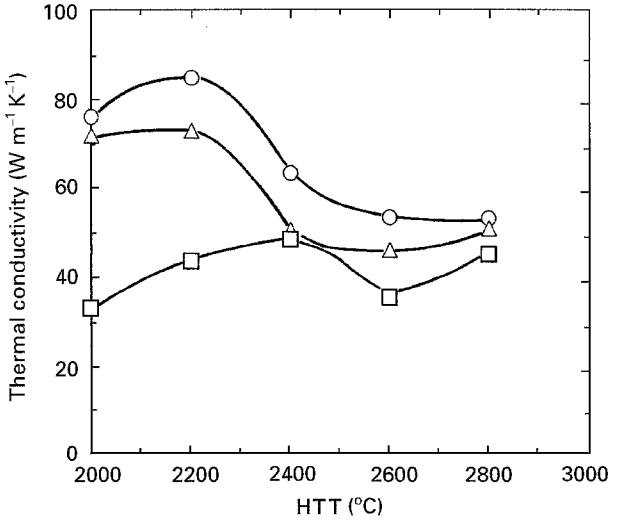

Figure 6 Effect of HTT on thermal conductivity at room temperature of (○) X-, (△) Y- and (□) Z-directions of boron-doped C–C composite.

TABLE III Air-oxidation loss at 800 °C for 3 h of the C–C composites with various HTTs

Sample code	HTT (°C)	Oxidation loss (mass %)
Boron-doped		
a	2000	9.9
b	2200	8.2
c	2400	2.2
d	2600	4.6
e	2800	5.3
Non-boron-doped		
f	2800	48.0

Air-oxidation loss of boron-doped and non-boron-doped C–C composites at 800 °C for 3 h are summarized in Table III. Oxidation loss of the composite is significantly reduced by boron-doping of 11.2 mass % at an HTT of 2800 °C. The composite whose HTT was 2400 °C was found to have the lowest oxidation loss of 2.2 mass %, 22 times lower than that of the non-boron-doped composite. This low oxidation loss at an HTT of 2400 °C must be responsible for the uniform distribution of boron, as shown in Fig. 1f. The cause of the reduction of oxidation loss for boron carbide-doped graphites at high temperatures was reported to be the formation of a boron oxide layer on the surface of the material, which was performed as an oxidation protection [19, 20]. Hence, uniform distribution of boron should be essential in order to attain thorough covering of the surface of the composite with an oxidation protective boron oxide layer, which may lead to suppression of oxidation loss.

Acknowledgement

The authors thank Professor Shiro Shimada, Hokkaido University and Dr Koji Kuroda, Toyo Tanso, for their lively discussions and encouragement, and Toyo Tanso R and D staff for their technical support. They also thank the Laboratory of Electron Probe Microanalyzer of Hokkaido University for EPMA measurements.

References

1. A. C. TITUS, in "Proceedings of Forth Conference on Carbon", edited by S. Mrozowski, M. L. Studebaker and P. L. Walker, Jr. (Pergamon Press, Oxford 1960) New York (1959) p. 703.
2. C. E. LOWELL, *J. Am. Ceram. Soc.* **50** (1967) 142.
3. R. E. WOODLEY, *Carbon* **6** (1968) 617.
4. R. B. TRASK, *Fuel* **47** (1968) 397.
5. D. J. ALLARDICE and P. L. WALKER Jr, *Carbon* **8** (1970) 375.
6. H. N. MURTY, D. L. BIEDERMAN and E.A. HEINTZ, *Fuel* **56** (1977) 305.
7. A.ŌYA, R.YAMASHITA and S. ŌTANI, *ibid.* **58** (1979) 495.
8. K. MIYAZAKI, K. KOBAYASHI and H. HONDA, *Tanso* **1977** (91) (1977) 121.

9. R. A. MURGATROYD and B. T. KELLY, *Atom. Energy Rev.* **15** (1977) 1.
10. K. FUJII, S.NOMURA, H. IMAI and S. SHINDO, in "Proceedings of a Specialists' Meeting", Tokai-mura, Japan, 9–12 September 1991, edited and published by International Atomic Energy Agency (IAEA) Wien, IAEA-TECDOC-690, pp. 169–76.
11. H. MATSUO, F. KOBAYASHI and K. SAWA, *Tanso* **1993** (159) (1993) 185.
12. Y. HIROOKA, R. W. CONN, R. CAUSEY, D. CROESSMANN, R. DOERNER, D. HOLLAND, M. KHANDAGLE, T. MATSUDA, G. SMOLIK, T. SOGABE, J. WHITLEY and K. WILSON, *J. Nucl. Mater.* **176, 177** (1990) 473.
13. T. HINO, M. HASHIBA, K. AKIMOTO and T. YAMASHINA, *J. Nucl. Sci. Technol.* **28** (1991) 20.
14. Y. HIROOKA, R. W. CONN, M. KHANDAGLE, G. CHEVALIER, T. SOGABE, T. MATSUDA, H. OGURA, H. TOYODA and H. SUGAI, *Fusion Technol.* **19** (1991) 2059.
15. T. HINO and T. YAMASHINA, *J. Nucl. Mater.* **196-198** (1992) 531.
16. T. HINO, K. ISHIO, Y. HIROHATA, T. YAMASHINA, T. SOGABE, M. OKADA and K. KURODA, *ibid.* **211** (1994) 30.
17. I. FUJITA, T. HINO, T. YAMASHINA, Y. KUBOTA, A. SAGARA, N. NODA, O. MOTOJIMA, T. MATSUDA, T. SOGABE, M. OKADA and K. KURODA, *J. Nucl. Mater.* **220-222** (1995) 795.
18. K. MIYAZAKI, T. HAGIO and K. KOBAYASHI, *Yougyo-Kyoukai- Shi* **86** (1978) 618.
19. K. MIYAZAKI, T. HAGIO and K. KOBAYASHI, *J. Mater. Sci.* **16** (1981) 752.
20. T. SOGABE, T. MATSUDA, K. KURODA, Y. HIROHATA, T. HINO and T. YAMASHINA, *Carbon* **33** (1995) 1783.
21. Y. NAKAJIMA, J. SAKAMOTO, K. KOBAYASHI, Y. UCHIYAMA and H. M. CHENG, in 'Proceedings of 19th Annual Meetings of Carbon Society of Japan", edited and published by The Carbon Society of Japan in Tokyo, 1992, Kyoto (1992) pp. 260–1.
22. S. RAGAN and G.T. EMMERSON, *Carbon* **30** (1992) 339.
23. M. INAGAKI, in "Tanso-zairyou-jikken-gijyutsu", edited by The Carbon Society of Japan (Kagakugijyutsu-sha, Tokyo, 1978) p. 55.
24. T. HAGIO, M. NAKAMIZO and K. KOBAYASHI, *Carbon* **27** (1989) 259.
25. R. M. BUSHONG and E. A. NEEL, in "Proceedings of 5th Conference on Carbon", edited by S. Mrozowski, M. L. Studebaker and P. L. Walker Jr. (Pergamon Press, Oxford) Pennsylvania **1** (1961) pp. 595–9.
26. S. MARINKOVIĆ, in "Chemistry and Physics of Carbon", Vol. 19, edited by P. A. Thrower (Marcel Dekker, New York, 1984) p. 1.

Received 18 October 1995
and accepted 21 May 1996